

Generation of reactive oxygen species by fungal NADPH oxidases is required for rice blast disease

Martin J. Egan, Zheng-Yi Wang, Mark A. Jones, Nicholas Smirnoff, and Nicholas J. Talbot*

School of Biosciences, Washington Singer Laboratories, University of Exeter, Perry Road, Exeter EX4 4QG, United Kingdom

Edited by Jeffrey L. Dangl, University of North Carolina, Chapel Hill, NC, and accepted by the Editorial Board May 19, 2007 (received for review January 23, 2007)

One of the first responses of plants to microbial attack is the production of extracellular superoxide surrounding infection sites. Here, we report that *Magnaporthe grisea*, the causal agent of rice blast disease, undergoes an oxidative burst of its own during plant infection, which is associated with its development of specialized infection structures called appressoria. Scavenging of these oxygen radicals significantly delayed the development of appressoria and altered their morphology. We targeted two superoxide-generating NADPH oxidase-encoding genes, *Nox1* and *Nox2*, and demonstrated genetically, that each is independently required for pathogenicity of *M. grisea*. $\Delta nox1$ and $\Delta nox2$ mutants are incapable of causing plant disease because of an inability to bring about appressorium-mediated cuticle penetration. The initiation of rice blast disease therefore requires production of superoxide by the invading pathogen.

appressorium | pathogen | plant disease | superoxide | virulence

One of the earliest manifestations of the plant defense response is the production of reactive oxygen species (ROS), including superoxide and its dismutation product, hydrogen peroxide (1). These ROS can kill pathogens directly (2) but also strengthen plant cell walls through the oxidative cross-linking of cell wall structural proteins (3) and may function in the regulation of programmed cell death (4). Although numerous studies have documented the detection of plant-derived ROS (2, 3, 5–7), very little is known about the role of ROS generation in invading plant pathogenic microorganisms. However, the recent discovery of functional members of the superoxide-generating NADPH oxidase (Nox) family within filamentous fungi (8) has led to increased speculation regarding the possible role of ROS in pathogenic species.

The most well characterized Nox remains that of the human phagocytic leukocyte, a multisubunit oxidase formed by the cytosolic regulatory components Rac, p67^{phox}, p47^{phox}, and p40^{phox} and the integral membrane protein flavocytochrome b₅₅₈, composed of the catalytic subunit gp91^{phox} and p22^{phox} (9). In activated macrophages, Nox enzymes induce K⁺ influx, causing pH changes in the phagocytic vacuole, leading to the killing of pathogens through activation of neutral proteases (10). Mutations in the catalytic gp91^{phox} subunit result in chronic granulomatous disease, an immunological disorder in which macrophages are unable to prevent the spread of infection (11). Plants contain enzymes that are homologous to gp91^{phox}, designated respiratory burst oxidase homologues (Rboh) (12). *Arabidopsis thaliana*, for example, possesses 10 Rboh isoforms involved in a diverse range of plant processes. ROS generated by the *A. thaliana* RHD2/RBOHC regulate root hair growth through the activation of Ca²⁺ channels (13), whereas RBOHD and RBOHF regulate stomatal closure, seed germination, and root elongation through abscisic acid signaling (14). Recent studies have shown that it is the activation of RBOHD and RBOHF that is responsible for ROS accumulation in several plant–microbe interactions (15). However, rather than driving programmed cell death as originally thought, ROS may actually antagonize salicylic acid-dependent prodeath signals (15).

In this article, we demonstrate a role for ROS in infection-related development of *Magnaporthe grisea*, the causal agent of rice blast disease, the most severe disease of cultivated rice

(*Oryza sativa*) (16). *M. grisea* causes plant infection by means of specialized infection structures called appressoria. These dome-shaped cells differentiate from the ends of fungal germ tubes in an elaborate process that is cell cycle-regulated and linked to programmed cell death of the fungal spore that initiates infection (17). Appressoria generate mechanical force to rupture the plant cuticle and gain entry to internal tissues (18, 19). Here, we provide cytochemical and pharmacological evidence that demonstrate the importance of ROS to the process of plant infection and rice blast disease. We also report the characterization of two potential sources for this ROS production, the *Nox1* and *Nox2* NADPH oxidases and demonstrate genetically that they are independently required for pathogenicity of *M. grisea*.

Results

The Rice Blast Fungus Generates ROS During Infection-Related Development. Rice blast disease is initiated by specialized infection cells called appressoria, swollen, dome-shaped cells that differentiate from the ends of a polarized germ tube and develop turgor pressure (18, 19) before producing a polarized infection hyphae that physically breaches the rice cuticle and invades the underlying epidermal cell. To determine the potential role of ROS in microbial pathogenicity, we first investigated the production of ROS during conidial germination and subsequent appressorium formation of *M. grisea* by using nitroblue tetrazolium (NBT), which forms a dark-blue water-insoluble formazan precipitate upon reduction by superoxide radicals (20).

Using this procedure, we were able to detect superoxide in conidia as early as 20 min after inoculation, as shown in Fig. 1A. Formazan precipitates were typically formed most intensely in the cell from which the germ tube emerged, although lighter staining was apparent in all cells of the spore. After ≈ 6 h of incubation, a dark formazan precipitate formed in the immature appressorium. These precipitates became less intense and more dispersed upon maturation, and, after 24 h, staining was restricted to the outer wall of appressoria. Incubation of conidia in diphenylene iodonium (DPI), a flavocytochrome inhibitor (21), before NBT reduction, appeared to abolish production of the formazan precipitate associated with sites of superoxide generation (Fig. 1B). Conidia incubated in NBT alone generated the previously observed patterns of staining. Conidia preexposed to the substrate inhibitor DPI, however, were translucent in comparison, showing no sign of staining (Fig. 1B). When considered together, the experiments suggested that superoxide was being generated enzymatically

Author contributions: N.J.T. designed research; M.J.E. and Z.-Y.W. performed research; Z.-Y.W., M.A.J., and N.S. contributed new reagents/analytic tools; M.A.J., N.S., and N.J.T. analyzed data; and M.J.E. and N.J.T. wrote the paper.

The authors declare no conflict of interest.

This article is a PNAS Direct Submission. J.L.D. is a guest editor invited by the Editorial Board.

Abbreviations: DPI, diphenylene iodonium; NBT, diphenylene iodonium; ROS, reactive oxygen species.

*To whom correspondence should be addressed. E-mail: n.j.talbot@exeter.ac.uk.

This article contains supporting information online at www.pnas.org/cgi/content/full/0700574104/DC1.

© 2007 by The National Academy of Sciences of the USA

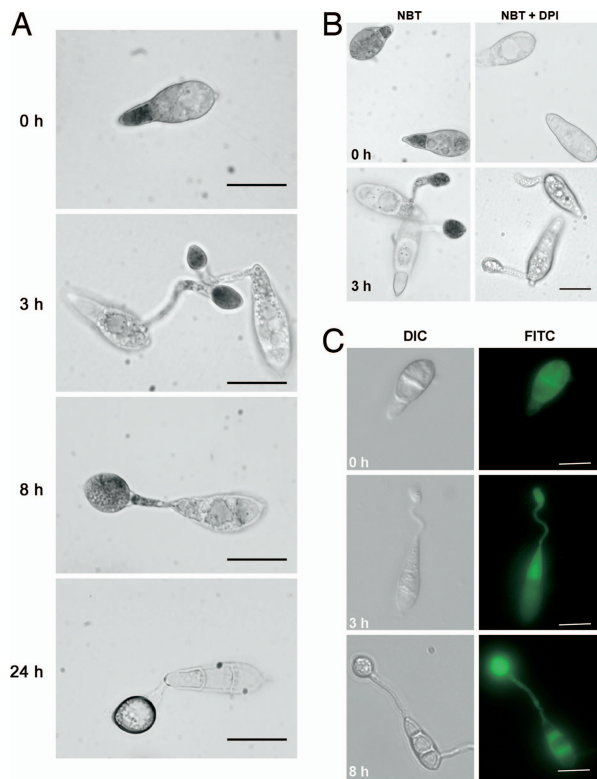


Fig. 1. ROS production during infection-related development of *M. grisea*. (A) Detection of superoxide by NBT staining during germination and appressorium formation in *M. grisea* strain Guy11. Conidia were inoculated on glass coverslips and incubated in a moist chamber at 26°C for 0, 3, 8, and 24 h before being stained with a 0.3 mM NBT aqueous solution for 20 min and viewed by bright-field microscopy. Representative bright-field images at each time point are shown. (B) Inhibition of *M. grisea* superoxide production by NADPH oxidase inhibitor diphenylene iodonium (DPI). Conidia were preincubated in a 25 μ M DPI solution for 20 min before NBT staining. (C) Detection of ROS by H₂DCFDA staining during infection-related development. Conidia were inoculated onto glass coverslips and incubated in a moist chamber at 26°C for 0, 3, and 8 h before being stained with a 2.5 μ g·ml⁻¹ carboxy-H₂DCFDA aqueous solution for 20 min and viewed by epifluorescence microscopy. (Scale bars, 10 μ m.)

within *M. grisea* infection structures, potentially by a flavoenzyme, such as a superoxide-generating NADPH oxidase.

To investigate production of other reactive oxygen intermediates, we used 2',7'-dichlorodihydrofluorescein diacetate (H₂DCFDA). This cell-permeable ROS indicator remains nonfluorescent until acetate groups are removed (H₂DCF) by intracellular esterases, and oxidation occurs within the cell to yield DCF. Although H₂DCF is primarily used for the detection of H₂O₂, DCFH (2', 7' dichlorofluorescein) can also be oxidized by other ROS such as hydroxyl radicals and nitric oxide. Superoxide, however, is thought incapable of oxidizing DCFH (see ref. 22). The localization pattern of ROS in infection structures based on this detection method was similar to that observed by NBT reduction, as shown in Fig. 1C. ROS production appeared to be highest within the cytoplasm of conidia before germination and were also present within the septal cell walls (Fig. 1C). As germination progressed, ROS localized to germ tubes (Fig. 1C) and a burst of ROS was frequently observed within incipient appressoria between 4 and 8 h after inoculation (Fig. 1C).

Infection-Related Development Is Delayed in *M. grisea* Conidia Exposed to Antioxidants. To investigate the role of ROS generated during germination and appressorium formation, conidia were germinated in either ascorbic acid, or Mn(III)tetrakis(1-methyl-4-

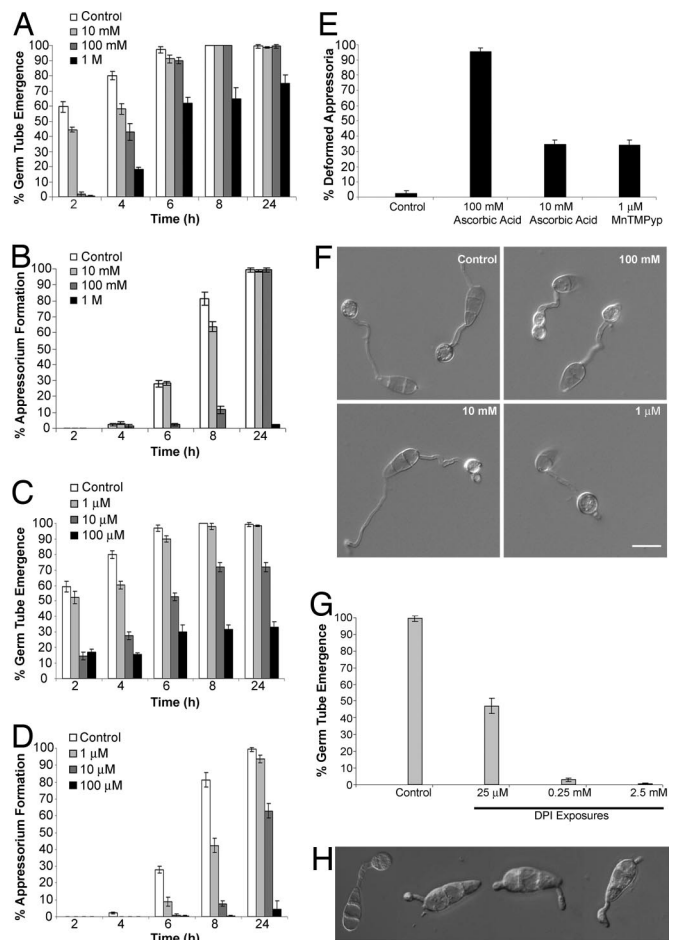


Fig. 2. Exposure to antioxidants inhibits infection-related development by *M. grisea*. (A–D) Bar charts showing the percentage of conidia able to germinate and form appressoria in the presence of 10 mM, 100 mM, and 1 M ascorbic acid, 2, 4, 6, 8, and 24 h after inoculation (A and B); 1 μ M, 10 μ M, and 100 μ M MnTMPyP, 2, 4, 6, 8, and 24 h after inoculation (C and D). (E) Bar chart showing the percentage of deformed appressoria resulting from exposure of germinating conidia to 100 mM ascorbic acid, 10 mM ascorbic acid, and 1 μ M MnTMPyP for 24 h. (F) Light micrographs showing appressorial deformities resulting from exposure to 100 mM ascorbic acid, 10 mM ascorbic acid, and 1 μ M MnTMPyP for 24 h. (Scale bar, 10 μ m.) (G) Bar chart showing the percentage of conidia able to germinate in the presence of 2.5 mM, 0.25 mM, and 25 μ M DPI after 24 h. (H) Light micrographs showing germ tube deformities resulting from exposure of conidia to 25 μ M DPI for 24 h.

pyridyl)porphyrin (MnTMPyP). Ascorbic acid has long been recognized as a potent scavenger of oxygen radicals (for review see ref. 23) whereas manganic porphyrins, such as MnTMPyP, have been routinely used as both superoxide dismutase and catalase mimics (24). Ascorbic acid affected conidial development in a dose-dependent manner, significantly delaying spore germination ($P < 0.002$) and appressorium formation ($P < 0.004$) at all experimental concentrations used, as shown in Fig. 2A and B. Germination and subsequent appressorium formation were similarly delayed in conidia exposed to MnTMPyP, yet at far lower doses than ascorbate (Fig. 2C and D).

More remarkable than the delay in germination caused by these antioxidants was the effect they exerted on appressorium morphology, as shown in Fig. 2E. Appressoria that were able to develop in the presence of antioxidants were often deformed, with more severe and frequent defects occurring at higher treatment concentrations (Fig. 2F). Over 95 \pm 2.5% of appressoria formed in 100 mM ascorbic acid were defective in their morphology. Typical

appressorial abnormalities included, “budding” (Fig. 2*F*) and attempts to repolarize (Fig. 2*F*). Our initial experiments showed that the flavoenzyme inhibitor DPI could prevent the production of superoxide during conidial germination and appressorium formation in *M. grisea*. However, the effect of this inhibition on conidial germination had not been investigated. Guy 11 conidia were therefore incubated in varying concentrations of DPI, and their development was assessed after 24 h. DPI had a dramatic effect on spore germination at all three experimental concentrations (Fig. 2*G*). Exposure to 25 μ M DPI approximately halved the number of conidia able to germinate compared with the control experiment (Fig. 2*G*). Concentrations of DPI in excess of 0.25 mM severely inhibited conidial germination, but were not lethal. Of those conidia that did germinate, all displayed aberrant germ tube morphology (Fig. 2*G*), and none were able to form appressoria.

NADPH Oxidases in the Rice Blast Fungus *M. grisea*. Cytological and pharmacological evidence indicated a potential role for ROS generation in infection-related development by *M. grisea*. To investigate this genetically, we set out to identify and characterize NADPH oxidases from *M. grisea*. NADPH oxidase-encoding genes are absent in ascomycete yeasts and the dimorphic basidiomycete fungi *Ustilago maydis* and *Cryptococcus neoformans*. Filamentous ascomycete fungi typically contain two NADPH oxidase (Nox) isoforms, based on analysis of recent genome sequences (25). The *M. grisea* genome (26), however, contains three putative NADPH oxidase-encoding genes, which we named *NOX1*, *NOX2*, and *NOX3*, which are homologous to *NoxA* and *NoxB* of *Aspergillus nidulans* (25), as shown in supporting information (SI) Fig. 5. Fungal Nox have been linked to both multicellularity (27) and cellular differentiation (25) and have been shown, genetically, to be necessary for development of sexual fruiting bodies (8, 28). More recently, Nox-derived ROS have been demonstrated to be critical in maintaining a mutualistic fungus–plant interaction (29, 30). We decided to test genetically whether *M. grisea* NADPH oxidases are responsible for production of ROS observed during conidial germination and appressorium formation and to elucidate the biological role of these superoxide-generating enzymes in the rice blast fungus.

To investigate the cellular function of *NOX1*, we performed a targeted gene replacement of the *NOX1* coding region with a 1.4-kb gene cassette bestowing resistance to the antibiotic hygromycin B. The gene replacement vector was introduced into a rice pathogenic strain of *M. grisea*, Guy 11, and hygromycin-resistant transformants were selected. DNA gel blot analysis identified four gene replacement mutants (see SI Fig. 6). To investigate the cellular function of *NOX2*, we performed a targeted gene deletion by introducing a 2.8-kb gene cassette bestowing resistance to the antibiotic sulfonyleurea into the coding region of *NOX2*, replacing 0.5 kb of the ORF as shown in Fig. 3*D* and *E*. The gene-replacement vector was introduced into both Guy 11 and the $\Delta nox1$ mutant background, and sulfonyleurea-resistant transformants were selected. DNA gel blot analysis identified three $\Delta nox2$ gene replacement mutants and three $\Delta nox1\Delta nox2$ double mutants (SI Fig. 6). To determine the effect of these mutations on *M. grisea* asexual development, mycelium was grown on standard growth medium (see *Materials and Methods*), and colony morphology and vegetative growth of the mutants were assessed. Accelerated hyphal growth was observed in $\Delta nox1$ mutants, and colonies displayed lighter pigmentation, whereas $\Delta nox2$ mutants grew normally, yet displayed increased aerial hyphal growth, giving colonies a white “fluffy” appearance (see SI Fig. 6). The $\Delta nox1\Delta nox2$ double mutants displayed the same accelerated vegetative growth phenotype of $\Delta nox1$ mutants. Although $\Delta nox1$ and $\Delta nox2$ mutants were not significantly affected in conidiogenesis, $\Delta nox1\Delta nox2$ mutants showed a dramatic reduction in conidiation (SI Fig. 6).

To investigate the expression and localization of Nox1 during infection-related development, we generated a C-terminal Nox1-

GFP fusion and introduced this construct into *M. grisea*. Conidia from *NOX1::GFP*-expressing strains were examined by epifluorescence microscopy. Faint GFP fluorescence was detected at the periphery of appressoria from ≈ 4 h, consistent with Nox1 being plasma membrane-localized (Fig. 3*A*). Previous attempts to localize other putative membrane proteins in *M. grisea*, such as Pth11p (31) and the tetraspanin-like protein Pls1p (32), resulted in the accumulation of the GFP fusion within appressorial vacuoles. It has been suggested (31) that this is a result of recycling of membrane proteins by endocytosis or from the partial missorting of the fusion protein. The detection of faint GFP fluorescence in the appressoria of *NOX1::GFP*-expressing strains after 24 h (Fig. 3*A*) is consistent with endocytic recycling.

Superoxide Production Is Altered in $\Delta nox1\Delta nox2$. To determine whether ROS production during appressorium differentiation was impaired in $\Delta nox1$, $\Delta nox2$, and $\Delta nox1\Delta nox2$ mutants, the extent of NBT reduction in these mutants was compared with that of the wild-type strain, Guy 11. No significant reduction in appressorium-specific superoxide production was detected in either $\Delta nox1$ or $\Delta nox2$ mutants (data not shown). However, the $\Delta nox1\Delta nox2$ mutant generated significantly less superoxide than Guy 11 during appressorium formation (Fig. 3*B*), as quantified by a reduction in the mean pixel intensity measurement because of accumulation of appressorium-localized formazan precipitates (Student's *t* test $P = 0.0145$) (Fig. 3*D*). In *M. grisea*, the oxidative burst associated with appressorium formation occurs as a highly transient, nonsynchronous event, making quantification challenging. However, several fungi have been shown to generate ROS during mycelial growth (28, 29), and we were interested to know whether ROS accumulation was affected vegetative hyphae of the Nox mutants, especially given the increased rate of hyphal elongation exhibited by the $\Delta nox1$ and $\Delta nox1\Delta nox2$ mutants. Guy 11 and the $\Delta nox1\Delta nox2$ mutant were grown on CM for 3 days and examined for superoxide production after 2 h of incubation in 0.05% (wt/vol) NBT. Formazan precipitates formed in the growing tips of Guy 11 and $\Delta nox1\Delta nox2$ hyphae in a process that was highly sensitive to DPI (Fig. 3*C*). Interestingly, quantitative analysis revealed a significant increase in superoxide production at the hyphal tips of the $\Delta nox1\Delta nox2$ mutant, when compared with those of Guy 11 (Student's *t* test $P < 0.001$) (Fig. 3*D*), suggesting up-regulation of an alternative source of ROS in the double Nox mutant. There was however, no detectable difference in superoxide production between Guy 11 and the $\Delta nox1$ and $\Delta nox2$ mutants (data not shown). Considered together, these results suggest the likely operation of numerous routes for cellular ROS generation in *M. grisea* during hyphal development and infection structure formation and highlight the specific role of Nox1 and Nox2 in developmentally regulated superoxide production during appressorium formation.

Nox1 and Nox2 Are Independently Required for Plant Infection. To determine the role of NADPH oxidases in plant disease, we inoculated seedlings of a blast-susceptible rice cultivar, CO-39 with four independently generated $\Delta nox1$ mutants, three independently generated $\Delta nox2$ mutants, and three $\Delta nox1\Delta nox2$ mutants. None of the Δnox mutants were able to cause disease on rice, and no lesions were observed even after prolonged incubation of the seedlings, as shown in Fig. 4*A*. Pathogenicity assays were repeated three times by using 60 rice seedlings per experiment, with uniform results. To ensure that the pathogenicity phenotypes were associated with loss of *NOX1* and *NOX2*, the respective genes were reintroduced and were able to restore the ability of *M. grisea* to cause disease (Fig. 4*A*). The ability of both $\Delta nox1$ and $\Delta nox2$ mutants to elaborate appressoria remained normal, but we observed by both light and transmission electron microscopy that appressorium-mediated cuticle penetration was completely absent in both *nox* mutants, as shown in Fig. 4*C–J*. Plant infection is therefore completely inhibited in $\Delta nox1$, $\Delta nox2$ and $\Delta nox1\Delta nox2$ mutants. Furthermore, $\Delta nox1$

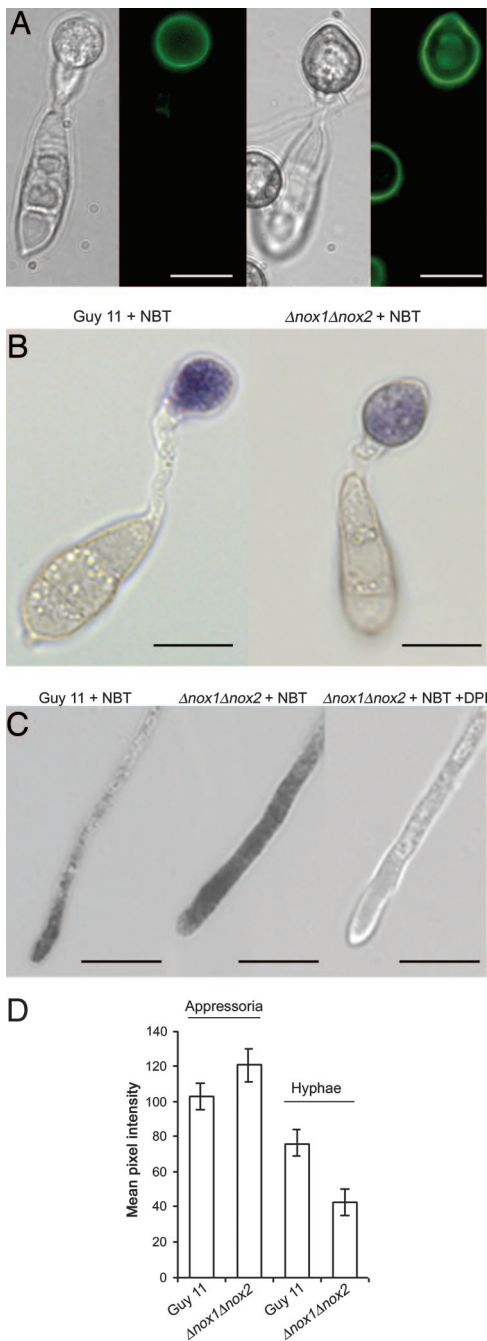


Fig. 3. Superoxide production is significantly altered in $\Delta nox1\Delta nox2$ mutants. (A) Cellular localization of Nox1-Gfp in *M. grisea*. A Guy 11 transformant expressing a *NOX1-GFP* fusion under the control of the *NOX1* promoter was inoculated onto glass coverslips and observed by epifluorescence microscopy. A faint fluorescence was observed at the appressorium periphery from 4 h. After 24 h, GFP was also detected in the central appressorium vacuole. (B) Detection of superoxide in the appressorium of Guy 11, and $\Delta nox1\Delta nox2$ mutants, by NBT staining. Conidia were inoculated on glass coverslips and incubated in a moist chamber at 26°C for 5 h before being stained with a 0.5% (wt/vol) NBT solution for 20 min and viewed by bright-field microscopy. (C) Detection of DPI-sensitive superoxide production in the hyphal tips of *M. grisea* strain, Guy 11, and $\Delta nox1\Delta nox2$ mutants by NBT staining. Colony mycelia were grown on CM media for 3 days and stained with 0.05% (wt/vol) NBT solution for 2 h in the presence and absence of 25 μ M DPI. (D) Bar chart showing mean pixel intensity in the appressorium and hyphal tips of Guy 11 and $\Delta nox1\Delta nox2$ mutants stained with NBT to detect superoxide (increased staining results in reduced pixel intensity and shorter bars, $n = 10$). Error bars indicate ± 2 SE. (Scale bars, 10 μ m.)

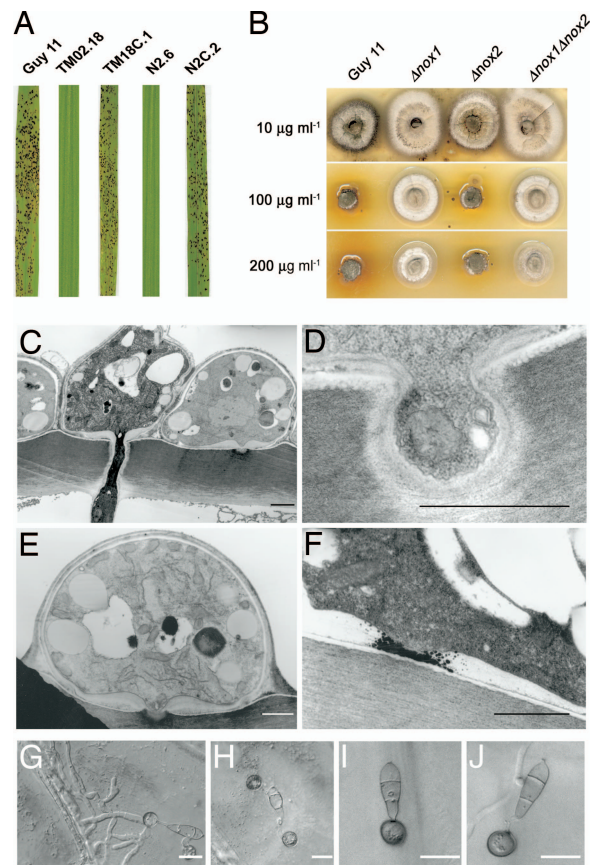


Fig. 4. $\Delta nox1$ and $\Delta nox2$ mutants are unable to cause rice blast disease. (A) Seedlings of rice cultivar CO-39 were inoculated with *M. grisea* conidial suspensions of identical concentration (1×10^5 conidia per ml^{-1}) of Guy11, the *nox1* mutant TM02.18, the *nox2* mutant N2.6, and the respective complemented strains TM18C.1 and N2C.2. Seedlings were incubated for 4 days for development of blast disease. (B) Mycelium from Guy11, $\Delta nox1$, $\Delta nox2$, and $\Delta nox1\Delta nox2$ mutants was inoculated onto complete medium containing calcofluor white at a concentration 10, 100, and 200 μ g- ml^{-1} and incubated at 24°C for 5 d with a 12-h light/dark cycle. (C–F) Transmission electron micrographs showing penetration hypha development (C) and cuticle penetration (D) by Guy 11 after 24 h on onion epidermis compared with appressorium of $\Delta nox1$ mutant (E) and attempted penetration point of $\Delta nox1$ mutant (F). (Scale bars, 1.0 μ m.) (G–J) Light micrographs representing the same developmental stages in Guy 11 (G), $\Delta nox1$ mutants (H), $\Delta nox2$ mutants (I), and $\Delta nox1\Delta nox2$ mutants (J). (Scale bars, 10 μ m.)

and $\Delta nox1\Delta nox2$ mutants failed to proliferate *in planta* even when inoculated onto wounded rice seedlings (data not shown), suggesting a requirement for Nox1 activity for *in planta* growth.

The oxidative cross-linking of cell wall components is well recognized in plants (33) but much less well known in fungi (34). We questioned whether superoxide produced by *M. grisea* Nox enzymes might function in fungal cell wall biogenesis, providing structural integrity to the appressorium during plant infection. Mycelium from Guy 11, $\Delta nox1$, $\Delta nox2$, and $\Delta nox1\Delta nox2$ were inoculated onto standard growth medium containing varying concentrations of calcofluor white, and their sensitivity was assessed after 5 days. Calcofluor white preferentially binds to polysaccharides containing 1,4-linked D-glucopyranosyl units and therefore alters the assembly of chitin microfibrils in fungi (35). The sensitivity against this compound is therefore closely related to the chitin content of cell walls. The $\Delta nox1$ and $\Delta nox1\Delta nox2$ mutants showed increased resistance to calcofluor white and were able to grow, unlike Guy 11 and $\Delta nox2$, on concentrations as high as 200 μ g- ml^{-1} calcofluor (Fig. 4B). We conclude that Nox1, but not Nox2, is necessary for correct cell wall biosynthesis.

Discussion

The release of ROS by plants is one of the first responses of plants to fungal invasion (36). In rice blast infections, for instance, plant-associated ROS have even been identified at the leaf surface after inoculation with *M. grisea* spores (37). In this article, we have shown that *M. grisea* spores also generate ROS during germination and formation of prepenetration-stage infection structures, in a process inhibited by the Nox inhibitor DPI. We identified the *M. grisea* genes *NOX1* and *NOX2* as potential sources of ROS production and, by targeted gene replacement, demonstrated that they are both required for fungal pathogenicity.

ROS and Fungal Cell Differentiation. The generation of ROS occurred at three distinct times in *M. grisea*, during conidial germination and appressorium development and during hyphal tip growth. In spores of the bread mold fungus *Neurospora crassa*, singlet oxygen is generated at the start of conidial germination (38), whereas ROS are required for germination of *Podospora anserina* ascospores (28). Here, we have shown that in *M. grisea*, spore germination and subsequent appressorium formation can be delayed, and to some extent inhibited, by exposure to the antioxidant ascorbic acid and the catalase mimic MnTMPyP. Exposure of *N. crassa* to water-soluble antioxidants was also shown to inhibit ROS and conidiation (38). Although we found $\Delta nox1$ and $\Delta nox2$ mutants to be unaffected in conidiogenesis, loss of both Nox enzymes led to a drastic reduction in spore production, consistent with the involvement of Nox-derived ROS in cellular differentiation. Significantly, the *M. grisea* $\Delta nox1\Delta nox2$ mutant showed a decrease in superoxide generation during appressorium formation but displayed increased ROS generation during hyphal growth. This is consistent with Nox1 and Nox2 being developmentally regulated during cellular differentiation and appressorium maturation but suggests that an additional means of ROS generation operates in *M. grisea* vegetative hyphae and is up-regulated as a consequence of the loss of Nox1 and Nox2. An alternative explanation for this observation could be that the altered cell wall structure of $\Delta nox1\Delta nox2$ mutants, suggested by their resistance to calcofluor white, may lead to increased permeability of hyphae to NBT and greater formazan precipitate accumulation. The presence of alternative sources of ROS generation in *M. grisea* may also explain why the morphological defects associated with appressorium development in the presence of DPI or antioxidants were not observed in Nox mutants. In *N. crassa*, the inactivation of catalase-3 has been shown to result in enhanced protein oxidation, higher carotene levels, hyphal adhesion, and higher amounts of aerial hyphae and conidia (39), whereas the lack of copper-zinc superoxide dismutase also increased carotene production and altered the polarity of the sexual fruiting bodies (40). These studies and our own observations provide an emerging body of evidence for the role of ROS in cellular differentiation by filamentous fungi (25).

NADPH Oxidases of the Rice Blast Fungus Are Essential for Plant Disease. In *M. grisea*, emergence of the penetration peg occurs by reestablishment of polar growth at the base of the appressorium in a direction orthogonal to the plant surface. Because $\Delta nox1$ and $\Delta nox2$ mutants appear incapable of appressorium-mediated cuticle penetration, it is worth speculating that Nox-derived ROS may regulate this dimorphic switch. In *Saccharomyces cerevisiae*, the reestablishment of polarity during bud emergence is known to involve GTPase Cdc42, which plays a key role in the transduction of polarity information to the morphogenetic machinery (41). In filamentous pathogenic fungi, such as *Colletotrichum trifolii*, Cdc42 is required for regulation of growth and development and is a negative regulator of appressorium formation (42). One may speculate that in the rice blast fungus, ROS, which have previously been implicated in the redox modification of regulatory proteins such as GTPases (43), may regulate appressorium maturation and the

reestablishment of polarity required for penetration peg formation and successful plant infection. In *C. trifolii*, ROS generation is regulated by Ras and Rac1 GTPases in a signaling pathway that may also require cytoplasmic phospholipase A2 (44) and is subject to negative regulation by Cdc42 (42). This signaling pathway is necessary for polarity, growth, and cellular differentiation in the fungus. In the mutualistic, endophytic fungus *Epichloë festucae*, ROS production via the *NoxA*-encoded NADPH oxidase is essential for mutualistic colonization of plant tissue, and its absence leads to premature senescence of host plants (29). ROS generation in *E. festucae* is regulated by a p67Phox-like regulator NoxR (30). When considered together, these studies and our own observations highlight the significance of ROS production to fungal development (25) and host-plant interactions.

Our study, however, also demonstrates that *M. grisea* Nox1 is involved in cell wall biochemistry. The deformities resulting from exposure of developing appressoria to antioxidants and the inability of $\Delta nox1$ and $\Delta nox2$ mutants to cause disease led us to test whether these mutations were a result of weakened cell walls. During plant infection, enormous turgor pressure is generated within *M. grisea* appressoria (18). To withstand such pressure, the appressorium has a highly differentiated cell wall, rich in chitin and containing a layer of melanin on its inner side (16, 18). It is feasible to hypothesize that Nox-derived ROS accumulate within the appressorium to facilitate oxidative cross-linking of proteins, hence strengthening the appressorium cell wall. The increased resistance of $\Delta nox1$ mutants to calcofluor white is consistent with such a role for Nox1 in cell wall biochemistry, particularly chitin biosynthesis or deposition (45). In *Caenorhabditis elegans*, Nox generated ROS are, for example, required for tyrosine cross-linking of the extracellular matrix (46). Exogenous application of H_2O_2 in soybean cells also causes the rapid insolubilization of two cell-wall structural proteins, ultimately leading to a strengthened cell wall (33). H_2O_2 could potentially play a similar role in appressoria, preparing the cell wall to resist pressures of up to 8.0 MPa produced during turgor generation (18). Melanin biosynthesis in *M. grisea* is an important component of appressorium formation (16), and melanin biosynthetic mutants are therefore nonpathogenic (16, 18). The lighter pigmentation of $\Delta nox1$ mutants also points to a potential role in melanin biosynthesis or deposition. Finally, the expression of *NOX1* during appressorium formation and the localization of Nox1 to the peripheral plasma membrane of appressoria is consistent with a role for the protein in cell wall differentiation required for plant infection.

Materials and Methods

Fungal Strains, Growth Conditions, and DNA Analysis. The growth and maintenance of *M. grisea*, media composition, nucleic acid extraction, and transformation were all as described (47). Gel electrophoresis, restriction enzyme digestion, gel blots, and sequencing were performed by using standard procedures (48).

Plant Infection Assays. Plant infection assays were performed by spraying seedlings of rice (*O. sativa*) cultivar CO-39 with a suspension of 10^5 conidia per ml^{-1} by using an artist's airbrush (47). Infection-related development was assessed by incubating conidia on plastic coverslips and allowing appressoria to form after 24 h. Cuticle penetration was measured as described (49).

ROS Detection Assay. For superoxide detection, *M. grisea* conidia were collected from 10- to 12-day CM agar plates in 3 ml of sterile deionized water and filtered through sterile Miracloth (Calbiochem, San Diego, CA) into a Falcon tube. Conidia were recovered by centrifugation at $5,000 \times g$ (JA-17; Beckman, Fullerton, CA) for 10 min at room temperature, and the pellet was resuspended in sterile deionized water to a final concentration of 10^5 conidia per ml^{-1} . A 100- μl droplet was placed onto a borosilicate glass coverslip (BDH, Poole, UK) and incubated in a moist chamber at 26°C for the desired time. At each time point, the water droplet was removed

from the coverslip and replaced with 200 μ l of a 0.05% (wt/vol) NBT aqueous solution and, where necessary, preincubated for 20 min with 25 μ M DPI (Sigma, St. Louis, MO). After incubation in NBT, the reaction was stopped by the addition of ethanol, and the pattern of formazan staining was observed by using a Axioskop 2 microscope (Zeiss, Thornwood, NY). Images were captured by using an AxioCam HR digital camera (Zeiss). The intensity of formazan precipitation in appressoria and hyphal tips was quantified by using AxioVision 4.6 image analysis software (Zeiss) to calculate mean pixel intensity within regions of interest fitted to the outline structure. Measurements were made on the most intensely stained spores and hyphae of each strain. Pixel intensity was reduced in areas of formazan precipitation.

For detection of ROS other than superoxide, conidia were prepared as above, and incubated in the presence of 2.5 μ g \cdot ml $^{-1}$ 5-(and 6)-carboxy-2',7'-dichlorodihydrofluorescein diacetate (carboxy-H₂DCFDA; Molecular Probes, Eugene, OR) except no NADPH was included. H₂DCFDA samples were observed by using a Zeiss Axioskop 2 fluorescence microscope using 495-nm excitation and 500- to 550-nm emission wavelengths.

NOX1 Genomic Cloning, Plasmid Construction, and Δ nox1 Complementation. The *A. thaliana* NADPH oxidase RbohA (50) was used to search the *M. grisea* genome database at the Broad Institute (Massachusetts Institute of Technology, Cambridge, MA) (www.broad.mit.edu/annotation/fungi/magnaporthe). The retrieved sequence was used to design primers BamHINOx1 (ATGGATCCGGTGCCCTCCTCAGTGCAGAA) and SpeINOx1 (ATACTAGTGTGGGGGTGAGAAGA). Italicized sequences here and below denote the restriction site introduced by a primer. BamHINOx1/SpeINOx1 were used to amplify a 3.98-kb fragment from *M. grisea* genomic DNA, consisting of the 1.89-kb NOX1 ORF and 1.05- and 1.04 kb flanks, which was then cloned into pGEM-T. Sequence analysis identified unique HindIII and XbaI restriction sites spanning the NOX1 ORF were used to remove a 1.85-kb portion of NOX1, which was replaced with a 1.40-kb fragment containing the *Hph* gene (51) to create pMJE1. The targeted gene replacement cassette was liberated from pMJE1 by digestion with BamHI and SpeI and was used to transform *M. grisea*.

For complementation of Δ nox1 mutants, primers 5'N1C (TAGCGGCCGCATTCTCGTTTGAGGCTGTAG) and 3'N1C

(ATTAGGATCCACCATCCGCTTCCCATTGTGTT) were used to amplify a 5-kb NOX1 genomic fragment, which was subsequently digested with NotI and BamHI, and ligated into pCB1532 (52). The resulting vector was transformed into the Δ nox1 background.

NOX2 Genomic Cloning, Plasmid Construction, and Complementation. Primers NOX2F (CAGCAGGCTCTGAATAAC) and NOX2R (CCCTGACCTGTTTCCTTCCA) were used to amplify a 3.98-kb fragment from *M. grisea* genomic DNA, consisting of the 1.95-kb NOX2 ORF and 300-bp and 1.74-kb flanks, which was then cloned into pGEM-T (Promega, Madison, WI). Sequence analysis identified two KpnI restriction sites within the NOX2 ORF, which were used to remove a 540-bp fragment. This was replaced with the *IVL1* gene, conferring resistance to sulfonylurea (52), to create pMJE2. NotI and ApaI restriction sites within the pGEM-T polylinker were used to liberate the gene disruption cassette from pMJE2. For Δ nox2 mutant complementation, primers 5'Nox2comp (GGGCAAGGCTGAATGAAAGAT) and 3'Nox2Comp (GTA-AATGGCTTGAAGACAGGG) were used to amplify a 5-kb NOX2 genomic fragment that was cloned into TOPO TA 2.1 (Invitrogen, Carlsbad, CA). HindIII and XbaI sites within the TOPO TA 2.1 polylinker were used to liberate the NOX2 fragment, which was subsequently cloned into pCB1003 containing the *hph* gene (51). The resulting vector was used to transform into the Δ nox2 mutant.

NOX1-GFP Fusion Plasmid Construction. Primers Nox1c-Tag 5'-ATGGCATTCTCGTTTGAGGCTCGTATA-3' and Nox1Age1 5'-ATACCGGTGAAATGCTCCTTCCAGAA-3' were used to amplify a 5-kb NOX1 genomic fragment that was cloned into TOPO TA 2.1 (Invitrogen) to create pNOX1. Primers GFP F 5'-CGACCCGGTATGGTGAGCAAGGGCGAG-3' and GFP R 5'-CGGGCCCGTGGAGATGTGGAGTGGG-3' were used to amplify the 1.4-kb sGFP construct and *TrpC* terminator sequence, which was subsequently cloned into pNOX1 by using AgeI and ApaI sites to create the pNOX1sGFP fusion. Primers SU F 5'-ATGGTACCGTCCGACGTGCCAACGCACAGT-3' and SU R 5'-ATGGTACCGTCCGACGTGAGAGCATGCAAT were used to amplify the 2.8-kb *IVL1* gene encoding resistance to sulfonylurea from the pCB1532 vector (52). The 2.8-kb *IVL1* fragment was ligated into the KpnI site within the polylinker of the TOPO TA 2.1 vector containing the NOX1GFP fusion.

- Wojtaszek P (1997) *Biochem J* 322:681–692.
- Levine A, Tenhaken R, Dixon R, Lamb CJ (1994) *Cell* 79:583–593.
- Bradley D, Kjellbom P, Lamb CJ (1992) *Cell* 70:21–30.
- Torres MA, Jones JD, Dangel JL (2005) *Nat Genet* 37:1130–1134.
- Doke N (1983) *Physiol Plant Pathol* 23:359–367.
- Apostol I, Heinstein PF, Low PS (1989) *Plant Physiol* 99:109–116.
- Nürnberg T, Nennstiel D, Jabs T, Sacks WR, Hahlbrock K, Scheel D (1994) *Cell* 78:449–460.
- Lara-Ortiz T, Riveros-Rosas H, Aguirre J (2003) *Mol Microbiol* 50:1241–1255.
- Diekmann D, Abo A, Johnstone C, Segal AW, Hall A (1994) *Science* 265:531–533.
- Reeves EP, Lu H, Jacobs HL, Messina CGM, Bolsover S, Gabella G, Potma EO, Warley A, Roes J, Segal AW (2002) *Nature* 416:291–297.
- Roos D, Deboer M, Kuribayashi F, Meischl C, Weening RS, Segal AW, Ahlin A, Nemet K, Hossle JP, Bernatowska-Matuszkiewicz E (1996) *Blood* 87:1663–1681.
- Torres M-A, Onouchi H, Hamada S, Machida C, Hammond-Kosack KE, Jones JDG (1998) *Plant J* 14:365–373.
- Foreman J, Demidchik V, Bothwell JHF, Mylona P, Miedema H, Torres M-A, Linstead P, Costa S, Brownlee C, Jones JDG (2003) *Nature* 422:442–446.
- Kwak JM, Mori IC, Pei ZM, Leonhardt N, Torres M-A, Dangel JL, Bloom RE, Bodde S, Jones JDG, Schroeder JI (2003) *EMBO J* 22:2623–2633.
- Torres M-A, Dangel JL, Jones JDG (2002) *Proc Natl Acad Sci USA* 99:517–522.
- Talbot NJ (2003) *Annu Rev Microbiol* 57:177–202.
- Veneault-Fourrey C, Barooah M, Egan M, Wakley G, Talbot NJ (2006) *Science* 312:580–583.
- Howard RJ, Bourett TM, Ferrari MA (1991) in *Infection by Magnaporthe grisea: An In Vitro Analysis*, eds Mendgen K, Lesemann DE (Springer, Berlin), pp 251–264.
- De Jong JC, McCormack BJ, Smirnov N, Talbot NJ (1997) *Nature* 389:244–245.
- Munkres K (1990) *Fungal Genet Newsl* 37:24–25.
- O'Donnell VB, Tew DG, Jones OTG, England PJ (1993) *Biochem J* 290:41–49.
- Zhu H, Bannenberg GL, Moldéus P, Shertzer HG (1994) *Arch Toxicol* 68:582–587.
- Smirnov N (2000) *Curr Opin Plant Biol* 3:229–235.
- Day BJ, Fridovich I, Crapo JD (1997) *Arch Biochem Biophys* 347:256–262.
- Aguirre J, Rios-Momberg M, Hewitt D, Hansberg W (2005) *Trends Microbiol* 13:111–118.
- Dean RA, Talbot NJ, Ebbole DJ, Farman ML, Mitchell TK, Orbach MJ, Thon M, Kulkarni K, Xu JR, Pan H, et al. (2005) *Nature* 434:980–986.
- Lalucque H, Silar P (2003) *Trends Microbiol* 11:9–12.
- Malagnac F, Lalucque H, Lepère G, Silar P (2004) *Fungal Genet Biol* 41:982–997.
- Tanaka A, Christensen MJ, Takemoto D, Park P, Scott B (2006) *Plant Cell* 18:1052–1066.
- Takemoto D, Tanaka A, Scott B (2006) *Plant Cell* 18:2807–2821.
- DeZwaan TM, Carroll AM, Valent B, Sweigard JA (1999) *Plant Cell* 11:2013–2030.
- Clergeot PH, Gourgues M, Cots J, Laurans F, Latorse MP, Pepin R, Tharreau D, Notteghem JL, Lebrun MH (2001) *Proc Natl Acad Sci USA* 98:6963–6968.
- Brisson LF, Tenhaken R, Lamb C (1994) *Plant Cell* 6:1703–1712.
- Tucker SL, Thornton CR, Tasker K, Jacob C, Giles G, Egan M, Talbot NJ (2004) *Plant Cell* 16:1575–1588.
- Elorza MV, Rico H, Sentandreu R (1983) *J Gen Microbiol* 129:1577–1582.
- Mellersh DG, Foulds IV, Higgins VJ, Heath MC (2002) *Plant J* 29:257–268.
- Pasechnik TD, Aver'yanov AA, Lapikova VP, Kovalenko ED, Kolomietz TM (1998) *Russ J Plant Physiol* 45:371–378.
- Hansberg W, de Groot H, Sies H (1993) *Free Radic Biol Med* 14:287–293.
- Michan S, Lledias F, Hansberg W (2003) *Eukaryot Cell* 2:798–808.
- Yoshida Y, Hasunuma KJ (2004) *J Biol Chem* 279:6986–6993.
- Chant J (1999) *Annu Rev Cell Dev Biol* 15:365–391.
- Chen C, Ha Y, Min J, Memmott SD, Dickman MB (2006) *Eukaryot Cell* 5:155–166.
- Adachi T, Pimentel DR, Heibeck T, Hou X, Lee YJ, Jiang B, Ido Y, Cohen RA (2004) *J Biol Chem* 279:29857–29862.
- Chen C, Dickman MB (2004) *Mol Microbiol* 51:1493–1507.
- Trilla JA, Durán A, Roncero CJ (1999) *Cell Biol* 145:1153–1163.
- Edens WA, Sharling L, Cheng G, Shapira R, Kinkade JM, Lee T, Edens HA, Tang X, Sullards C, Flaherty DB, et al. (2001) *J Cell Biol* 154:879–891.
- Talbot NJ, Ebbole DJ, Hamer JE (1993) *Plant Cell* 5:1575–1590.
- Sambrook J, Fritsch EF, Maniatis T (1989). *Molecular Cloning: A Laboratory Manual* (Cold Spring Harbor Lab Press, Cold Spring Harbor, NY).
- Chida T, Sisler HD (1987) *J Pesticide Sci* 12:49–55.
- Keller T, Damude HG, Werner D, Doerner P, Dixon RA, Lamb C (1998) *Plant Cell* 10:255–266.
- Carroll AM, Sweigard JA, Valent B (1994) *Fungal Genet Newsl* 41:22.
- Sweigard J, Chumley F, Carroll A, Farrall L, Valent B (1997) *Fungal Genet Newsl* 44:52–53.